Properties of Small-Ring Free Radicals. 2. Thermal Decomposition of Alicyclic Percarboxylates

Richard A. Wolf,* Michael J. Migliore, Patrick H. Fuery, Paul R. Gagnier, Isidore C. Sabeta, and Richard J. Trocino

Contribution from the Department of Chemistry, State University College, New Paltz, New York 12562. Received April 27, 1978

Abstract: A series of *tert*-butyl alicyclic percarboxylates (**1–5**) was synthesized, and the rate constants for their thermal decomposition in hydrocarbon solvents were measured at several temperatures. Deuterium isotope effects, solvent viscosity effects, activation parameter analyses, and reactivity–selectivity principle analyses suggest that the mechanism of thermolysis shifts from stepwise (**1**) to essentially concerted, two-bond cleavage (**4 and 5**) as the alicyclic ring is made larger. At higher initial perester concentrations, and in the absence of free-radical scavenger, the 1-H-alicyclic peresters suffer considerable radical-induced decomposition, with some attack at the α hydrogen. Attempts were made to determine the rate constants for the radical-induced modes of decomposition. The results of these studies have implications regarding the effect of structure on rates of perester thermolyses and other related radical-forming reactions.

Introduction

The relative rates of radical-forming reactions have traditionally been rationalized in terms of the relative stabilities of the radicals being formed, and hence in terms of the relative stabilities of the partially radical-like transition states. Rüchardt has challenged this interpretation for many radical-forming reactions, suggesting that differences in ground (reactant) state energies may account for the observed rate differences.[1] For example, Rüchardt asserts that the rates of thermal decomposition of peresters are determined mainly by polar and to a lesser extent by steric effects, proposing that in the transition state the O–O bond is essentially broken, but the $C(\alpha)$–C(carbonyl) bond is only slightly stretched. A significant amount of the justification for this picture is based on the relative rates observed for thermolysis of several alicyclic and polycyclic percarboxylates.[2] The thermolyses of symmetric diazenes[3] and solvolysis (carbenium ion forming) reactions, on the other hand, appear to have transition states with properties similar to products.

Subsequently, similar transition states have been proposed for several other related reactions, including the photoinduced decomposition of hypochlorites,[2] the oxidation of alkylphenylmethanols by ceric ammonium nitrate,[4] the photochemical α-cleavage of deoxybenzoins,[5] and the photoinduced decarboxylation of acyl hypoiodites.[6] Effects of ring size similar to perester thermolysis on rates of reactions have also been observed for the thermolysis of bisalicyclic acyl peroxides,[7] relative reactivities of C–H bonds toward chlorine atom abstraction,[8] and rates of decarbonylation of alicyclic acyl radicals.[9]

Although Rüchardt's ideas regarding the mechanism of perester decomposition are based on some solid scientific grounds (which will be discussed later), they are also based partially on the assumption of a *common* mechanism (presumably concerted, two-bond cleavage) of perester thermolysis for almost all peresters, except those whose decomposition Rüchardt felt would lead to unusually unstable radicals (like phenyl or 1-norbornyl). We investigated more closely the mechanism(s) of thermal decomposition of the series of alicyclic peresters shown in Chart I, in order to assess the validity of the direct comparison of observed rate constant values for perester thermolysis with the rates of the other radical-forming reactions cited above. For this study we used rates of decomposition, viscosity effects, deuterium isotope effects, Arrhenius parameters, and reactivity–selectivity arguments.

Results

The first-order rate constants for thermal decomposition of

Chart I. *tert*-Butyl Alicyclic Percarboxylates
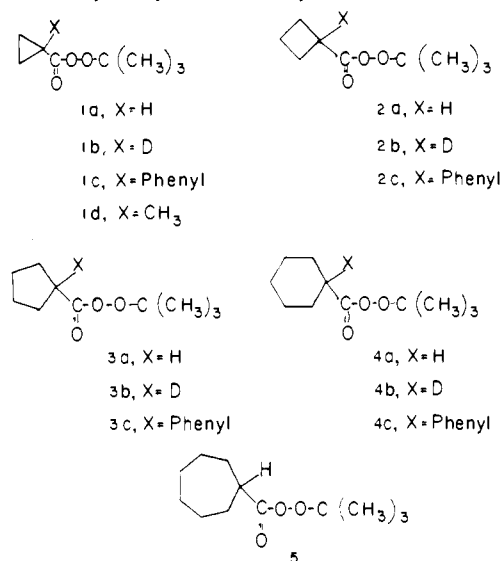
peresters **1–5** are given in Tables I and II. Under the conditions of hydrocarbon solvent, low initial perester concentration, and addition of radical scavenger, the kinetic measurements fit a straight line linear least-squares plot for the first-order kinetic expression. The kinetics were determined by measuring the rates of disappearance of the carbonyl stretching peaks for the peresters at 1780 cm^{-1} (see Experimental Section). No curvature was detected in the first-order rate constants of thermolysis (Tables I and II) for determinations through 3–4 half-lives of reaction. The correlation coefficients for each kinetic plot were greater than 0.999. Standard errors of each linear slope were uniformly less than the standard deviations from the average values of rate constants from several kinetic runs done at the same conditions. The average rate constants expressed in Tables I and II are the results of repeated determinations using, for each perester, different batches of perester, different batches of styrene, and different batches of solvent. All peresters were purified immediately prior to sealing up the kinetic solutions. All solvents were distilled (except for squalane). The percent of deuterium incorporation at the 1 position was determined for each perester **1b–4b** by NMR integration and by mass spectrometry (see Experimental Section). The
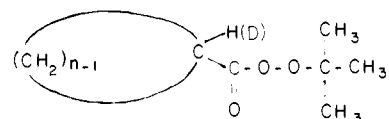
Table I. Rate Constants and α Secondary Deuterium Isotope Effects for the Thermolysis of 1-H(D) Peresters

perester	solvent[a]	temp, °C	$k \times 10^4$, s^{-1} [b]	k_H/k_D [c]
1a	C-8	120.4	1.505 ± 0.008	1.005 ± 0.010
1a	C-8	113.0	0.619 ± 0.009	1.011 ± 0.021
1a	C-12	113.0	0.548 ± 0.005	
1a	C-16	113.0	0.492 ± 0.002	
1a	C-8	102.6	0.171 ± 0.001	1.002 ± 0.005
1a	C-16	102.6	0.128 ± 0.002	
2a	C-8	113.0	1.668 ± 0.032	
2a	C-8	102.6	0.484 ± 0.002	0.997 ± 0.014
2a	C-16	102.6	0.433 ± 0.004	
2a	C-8	92.9	0.121 ± 0.001	1.015 ± 0.013
3a	C-8	113.0	2.89 ± 0.12	
3a	C-16	113.0	3.02 ± 0.10	
3a	C-8	102.6	0.887 ± 0.007	1.058 ± 0.040
3a	C-8	92.9	0.247 ± 0.004	1.040 ± 0.026
4a	C-8	113.0	6.58 ± 0.07	1.047 ± 0.016
4a	C-8	102.6	2.026 ± 0.007	1.043 ± 0.010
4a	C-16	102.6	2.046 ± 0.003	1.072 ± 0.019
4a	sq	102.6	2.048 ± 0.029	
4a	C-7	102.6	1.999 ± 0.020	1.062 ± 0.020
4a	C-8	92.9	0.613 ± 0.007	1.053 ± 0.026
4a	C-16	92.9	0.620 ± 0.011	1.067 ± 0.027
4a	C-8	82.2	0.157 ± 0.001	1.057 ± 0.017
5	C-8	102.6	5.07 ± 0.17	
5	C-16	102.6	5.17 ± 0.16	
5	C-8	92.9	1.703 ± 0.028	
5	C-16	92.9	1.801 ± 0.028	

[a] C-8 = 2,2,4-trimethylpentane; C-12 = *n*-dodecane; C-16 = *n*-hexadecane; sq = squalane; C-7 = *n*-heptane. [b] Initial concentrations of peresters are 0.010–0.020 M. Initial concentrations of styrene are 0.15–0.20 M. The rate constants are the average of results from four to eight kinetic runs at each temperature for each solvent. Errors are standard deviations from the average. [c] Corrected to 100% D. Errors are standard deviations.

Table II. Rate Constants for the Thermolysis of 1-Substituted Peresters

perester	solvent[a]	temp, °C	$k \times 10^4$, s^{-1} [b]
1c	C-8	120.4	2.04 ± 0.06
1c	C-8	113.0	0.896 ± 0.006
1c	C-12	113.0	0.867 ± 0.006
1c	C-8	102.6	0.253 ± 0.002
1d	C-8	113.0	0.747 ± 0.011
1d	C-8	102.6	0.230 ± 0.003
2c	C-8	61.6	2.46 ± 0.10
2c	C-8	52.3	0.769 ± 0.027
2c	C-12	52.3	0.789 ± 0.010
2c	C-16	52.3	0.880 ± 0.028
3c	C-8	52.3	3.51 ± 0.18
3c	C-8	43.5	1.184 ± 0.055
4c	C-8	61.6	12.18 ± 0.14
4c	C-8	52.3	3.91 ± 0.02
4c	C-8	43.5	1.27 ± 0.04

[a] See footnote *a*, Table 1. [b] See footnote *b*, Table 1.

Table III. Activation Parameters for the Thermolysis of Peresters

perester	solvent[a]	$\Delta H^\ddagger$, kcal/mol[b]	$\Delta S^\ddagger$, cal/deg·mol[b]
1a	C-8	34.9 ± 0.5	12.0 ± 1.2
1a	C-16	36.7 ± 0.4	16.2 ± 1.1
1c	C-8	33.7 ± 0.6	9.7 ± 1.5
1d	C-8	31.9 ± 0.8	4.6 ± 2.0
2a	C-8	35.9 ± 0.4	16.7 ± 1.0
2c	C-8	26.4 ± 1.8	3.7 ± 5.3
3a	C-8	33.6 ± 0.8	11.8 ± 2.2
3c	C-8	24.7 ± 2.3	1.2 ± 7.1
4a	C-8	32.4 ± 0.3	10.3 ± 0.5
4a	C-16	32.6 ± 0.5	11.0 ± 1.5
4c	C-8	25.7 ± 0.5	4.6 ± 1.5
5	C-8	30.0 ± 1.4	5.8 ± 3.8
5	C-16	29.0 ± 1.3	3.1 ± 3.5

[a] See footnote *a*, Table 1, for explanation of symbols. [b] Errors are propagated from standard deviations of rate constants.

deuterium isotope effects expressed in Table I have been corrected to 100% deuterium at position 1.

The activation parameters ($\Delta H^\ddagger$ and $\Delta S^\ddagger$) for the thermolysis of each perester have been calculated and have been listed in Table III. The errors cited are calculated from propagations of the standard deviations of the rate constants from the highest and lowest temperatures in each series. In all cases these errors are larger than the standard errors of the slopes, when three or more temperatures were investigated. The propagation of errors method seems the fairest estimate of real errors in these activation parameters.

The effect of changing the viscosity of the paraffin solvent (while maintaining essentially constant polarity) was determined in order to measure the possibility of solvent "cage effects" on the thermolysis of these peresters. The ratios of rate constants in "standard" solvent (i.e., 2,2,4-trimethylpentane) to rate constants in "thick" or viscous solvents are expressed in Table IV. Table V contains some estimates of individual rate constants from the Pryor equation for solvent viscosity effects[10] (see Discussion section).

Some comparisons of relative rate constants for our perester series with other peresters are made in Table VI. Table VII contains a summary of relative rate constants, total α deuterium isotope effects (averaged over all temperatures for each perester 1a–4a), and total hexadecane solvent viscosity effects (averaged over all temperatures).

Although reproducible, straight-line first-order kinetic plots are obtained for all these peresters under conditions of low initial perester concentration and addition of radical scavenger (styrene), the quality of these plots deteriorated under other experimental conditions. Thus, if higher initial perester concentrations (0.20 M, compared to 0.02 M) were used and if no radical scavenger were added, the "first-order" rate constants

measured were higher than those measured at "standard" conditions, gave downward curvature throughout the $-\ln$ (perester) vs. time plots, and were generally much less reproducible. All peresters with proton or deuterium at the 1 position (α carbon) behaved in this way. A few individual rate constants for the thermolysis of 4a (4b) are given in Table VIII as an example of the concentration and scavenger effect.

Product studies were not attempted in these studies, since products for these same peresters (except for series 1b–4b) were determined by Rüchardt.[2,16] Rüchardt measured high CO_2 yields, approaching 100% for these peresters. No untoward products were detected by Rüchardt.

Discussion

The two commonly operating mechanisms for the thermal decomposition of *tert*-butyl peresters under nonpolar solvent conditions are given in Scheme I.[17] Contributions to the decomposition pathways by ionic mechanisms ("Criegee"-type reactions[18] or carboxy inversions[19]) can probably be ruled out on the basis of product studies, high CO_2 yields, and the use of nonpolar solvents. Contributions from radical-induced decomposition of peresters, which might lead to complicated kinetic expressions[20] appear not to be operating under the conditions used to obtain the data in Tables I–IV (more on this later).
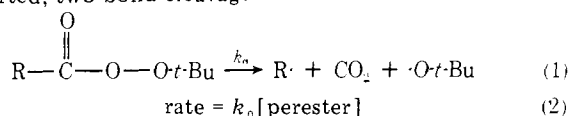
Under the conditions of low initial perester concentrations (0.01–0.02 M) and added styrene (0.15–0.20 M), we believe that the peresters in series 1–5 undergo thermal decomposition by the concerted or stepwise mechanisms shown in Scheme I.

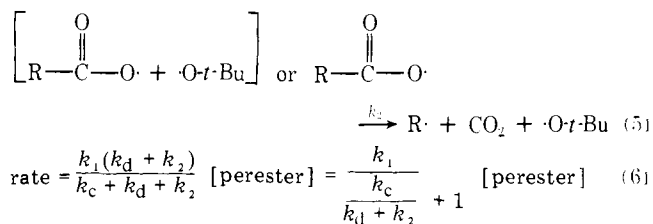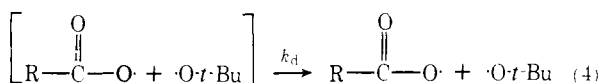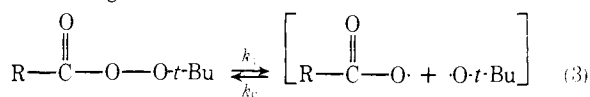**Table IV.** Solvent Viscosity Effects for Thermal Decomposition of Peresters

perester	temp, °C	thick solvent[a]	η_{Th}/η_{C-8}[b]	$k(C-8)/k(Th)$[c]
1a	113.0	C-16	4.12	1.26 ± 0.02
1a	113.0	C-12	2.43	1.13 ± 0.02
1a	102.6	C-16	4.29	1.34 ± 0.02
1c	113.0	C-12	2.43	1.03 ± 0.02
2a	102.6	C-16	4.29	1.12 ± 0.02
2c	52.3	C-12	2.90	0.97 ± 0.05
2c	52.3	C-16	5.47	0.87 ± 0.06
3a	113.0	C-16	4.12	0.95 ± 0.08
4a	102.6	C-16	4.29	0.99 ± 0.01
4a	102.6	sq		0.99 ± 0.02
4a	102.6	C-7	1.02	1.01 ± 0.01
4a	92.9	C-16	4.47	0.98 ± 0.03
5	102.6	C-16	4.29	0.98 ± 0.06
5	92.9	C-16	4.47	0.95 ± 0.03

[a] See footnote *a*, Table 1, for explanation of symbols. [b] Calculated from $\eta = A_v \exp(E_v/RT)$ from data in Ph.D. Dissertation of Kennedy Smith, Louisiana State University, 1969, p 15. η_{Th}/η_{C-8} is the ratio of viscosities of thick solvent to viscosity of 2,2,4-trimethylpentane. [c] Ratio of first-order rate constants for thermolysis of perester in 2,2,4-trimethylpentane to rate constants in thick solvent. Errors are propagated from standard deviations of rate constants.

Scheme I
concerted, two-bond cleavage

$$R-\overset{\overset{O}{\|}}{C}-O-O\text{-}t\text{-Bu} \xrightarrow{k_a} R\cdot + CO_2 + \cdot O\text{-}t\text{-Bu} \quad (1)$$

$$\text{rate} = k_0[\text{perester}] \quad (2)$$

stepwise cleavages

$$R-\overset{\overset{O}{\|}}{C}-O-O\text{-}t\text{-Bu} \underset{k_c}{\overset{k}{\rightleftharpoons}} \left[R-\overset{\overset{O}{\|}}{C}-O\cdot + \cdot O\text{-}t\text{-Bu}\right] \quad (3)$$

$$\left[R-\overset{\overset{O}{\|}}{C}-O\cdot + \cdot O\text{-}t\text{-Bu}\right] \xrightarrow{k_d} R-\overset{\overset{O}{\|}}{C}-O\cdot + \cdot O\text{-}t\text{-Bu} \quad (4)$$

$$\left[R-\overset{\overset{O}{\|}}{C}-O\cdot + \cdot O\text{-}t\text{-Bu}\right] \text{ or } R-\overset{\overset{O}{\|}}{C}-O\cdot$$

$$\xrightarrow{k_2} R\cdot + CO_2 + \cdot O\text{-}t\text{-Bu} \quad (5)$$

$$\text{rate} = \frac{k_1(k_d + k_2)}{k_c + k_d + k_2}[\text{perester}] = \frac{k_1}{\dfrac{k_c}{k_d + k_2} + 1}[\text{perester}] \quad (6)$$

Table V. Comparison of Component Rate Constants in Viscosity Expression[a]

perester	temp, °C	$k_1 \times 10^5$, s^{-1}	k_c/A_D
1a	113.0	8.02 ± 0.33	0.077 ± 0.009
1a	102.6	2.41 ± 0.07	0.103 ± 0.010
2a	102.6	5.37 ± 0.10	0.028 ± 0.004

[a] Component rate constants calculated using eq 7 with $\alpha = 0.5$.

Table VI. Relative Rate Constants for Thermal Decomposition of Some Peresters

perester	solvent[a]	$k(\text{rel})$[b]	ref
1a	C-8	0.087	c
1d	C-8	0.117	c
2a	C-8	0.238	c
3a	C-8	0.437	c
4a	C-8	1.02	c
5	C-8	2.57	c
$(CH_3)_2CHCO_3$-t-Bu	C-8	(1)	d
$CH_3CH_2CO_3$-t-Bu	ethylbenzene	0.0095	e
CH_3CO_3-t-Bu	cumene	0.12	f
$(CH_3)_3CCO_3$-t-Bu	cumene	21.4, 13.4	g,h

[a] See footnote *a*, Table 1, for explanation of symbol. [b] Relative rate constant at 103.4 °C. Rate constants calculated from published activation parameters. [c] This work. [d] Reference 11. [e] Reference 12. [f] Reference 13. [g] Reference 14. [h] Reference 15.

Table VII. Summary of Relative Rate Constants, Deuterium Isotope Effects, and Solvent Viscosity Effects for Thermolysis of 1-H(D)-Peresters

perester	$k(\text{rel})$, 102.6 °C[a]	k_H/k_D	$k(C-8)/k(C-16)$[b]
1a	(1)	1.006 ± 0.005	1.30 ± 0.04[c]
2a	2.83	1.006 ± 0.009	1.12 ± 0.02[d]
3a	5.18	1.049 ± 0.009	0.95 ± 0.08[e]
4a	11.8	1.050 ± 0.006	0.99 ± 0.01[f]
5	29.6		0.96 ± 0.02[f]

[a] In 2,2,4-trimethylpentane solvent. Initial perester concentrations are 0.01–0.02 M. Initial styrene concentrations are 0.15–0.20 M. Errors are standard deviations from the value averaged over all temperatures. Actual errors are undoubtedly higher (see Table I). [b] Ratio of rates in 2,2,4-trimethylpentane to rates in *n*-hexadecane. [c] Average of results at 113.0 and 102.6 °C. Error is standard deviation from value averaged over two temperatures. [d] Results at 102.6 °C. [e] Results at 113.0 °C. [f] Average of results at 102.6 and 92.9 °C. Error is standard deviation from value averaged over two temperatures.

Distinguishing between Concerted and Stepwise Mechanisms. Separating the concerted and stepwise mechanisms for perester thermolysis has been accomplished in the past by various mechanistic probes. These probes include deuterium isotope effects,[11,21] solvent viscosity effects,[10,22,23] activation parameter analysis,[24-26] volumes of activation,[27] and oxygen-18 scrambling studies.[23b,28] Rüchardt cites the high yield of CO_2 and the absence of oxygen-18 scrambling in recovered 1a and 4a as evidence against the operation of the stepwise mechanism.[16] However, the yield of CO_2 is not a reliable mechanistic probe (concerted vs. stepwise) since the rate of decarboxylation (reaction 5 in Scheme I) is known to be fast, relative to H-atom abstraction by $RCO_2\cdot$, for R = alkyl.[29] Only peresters whose decomposition would lead to geometrically and/or electronically destabilized radicals give significant carboxylic acid products. For example, moderate yields of cycloalkanecarboxylic acids are obtained from thermolysis of *tert*-butyl cyclopropanepercarboxylates (1-F, Cl, OCH_3, or Br)[30] and *tert*-butyl 7-fluoro- and 7-chloro-*endo*- and -*exo*-norcarane-7-percarboxylates.[31]

Evidence already exists for the different mechanistic behavior of 1a vs. 4a. On the basis of volumes of activation measurements, Neuman concluded that 4a undergoes thermal decomposition by the concerted mechanism.[27a] The isolation of 1a from the thermal decomposition of *N*-nitroso-*N*-*tert*-butoxycyclopropanecarboxamide strongly suggests that the cyclopropanecarboxyl radical is relatively long lived (at least with respect to its ability to combine with *tert*-butoxy radical). Thus, Koenig's elegant experiments suggest that 1a undergoes thermal decomposition by the stepwise pathway.[32]

Two features of the perester series 1a–4a stand out as being anomalous. The first anomaly is the effect of ring size on the rates of thermolysis of the alicyclic percarboxylates. As already noted by Rüchardt,[1] the ring size trends for the perester thermolysis do not follow the trends for carbenium ion forming reactions,[1,33,34] for carbanion-forming reactions,[35] or for thermolysis of symmetric bisalicyclic diazenes.[2,36] The carbenium ion forming reactions and diazene thermolyses are thought to have transition states with product-like character. Carbenium ions, and to a lesser extent free radicals, supposedly require planar central carbons, thus explaining the slow rates

Table VIII. Effect of Initial Perester and Scavenger
Concentrations on Some Rates of Thermolysis and α Deuterium
Isotope Effects for **4a** (**4b**)

run	$[4a]_0{}^a$	$[styrene]_0{}^b$	$k \times 10^4, s^{-1}\,{}^c$	$k_H/k_D{}^d$
3	0.020	0.050	2.01	1.04
8	0.020	0.151	2.01	1.04
65	0.020	0	2.09	1.10
74	0.160	0	2.54	1.28
75	0.320	0	3.14	1.30

a Initial concentration of **4a** in moles/liter, 2,2,4-trimethylpentane solvent. *b* Initial concentration of styrene in moles/liter. *c* First-order rate constant measured for first half-life of reaction, at 102.6 °C, in 2,2,4-trimethylpentane solvent. *d* α deuterium isotope effect, calculated from overall rate constants of **4b** measured simultaneously to, and under the same experimental conditions of, the corresponding **4a**. Isotope effects have been corrected to 100% D.

for the cyclopropyl, cyclobutyl, and cyclohexyl members of these series. The requirement for strict planarity at the central carbon atom for carbenium ions has recently been challenged, however,[37] as has the planar requirements of the central carbon of free radicals.[38-40]

The second anomaly is the relatively small changes in the magnitudes of the overall rate constants upon changing from **1a** to **4a**. Thus, only a one order of magnitude change in rate constant is exhibited in going from the apparently stepwise mechanism (**1a**) to the apparently concerted mechanism (**4a**) (see Table VI). This suggests a very subtle crossover in mechanism for this series and makes clear the need for investigating the mechanisms of thermal decomposition for the alicyclic perester series more carefully.

Rüchardt's measured rate constants, in ethylbenzene solvent, are uniformly higher (except for **1a**) than the rate constants measured by us (40% higher, on the average, at the same temperature). There have been suggestions in the literature that aromatic solvents accelerate the thermal decomposition of diacyl peroxides (as compared to thermolysis in paraffin solvents) by the more polarizable aromatic solvents engaging in partial charge-transfer complex formation with the peroxide.[41,42] We believe that these possible ionic complications in the thermolysis of peresters should be avoided by the use of paraffin solvents instead of aromatic solvents.

We believe that the data in Tables I-IV, summarized in Table VII, support the proposal that **1a** and **2a** undergo thermal decomposition primarily by the stepwise mechanism and that **3a**, **4a**, and **5** undergo thermal decomposition primarily by the concerted mechanism. Furthermore, we believe that the alicyclic peresters of intermediate ring size (such as **2a** and **3a**) have components of both mechanisms in their decomposition pathways.

Activation Parameters. On the basis of a Polanyi plot of $\Delta H^{\ddagger}$ vs. $\Delta H°$, Richardson and Koskinen suggested that peresters undergoing thermolysis with $\Delta H^{\ddagger}$ less than 30 kcal/mol will do so via the concerted mechanism.[26] Conversely, peresters undergoing thermolysis with $\Delta H^{\ddagger}$ more than 33 kcal/mol will supposedly do so via the stepwise mechanism. Pryor set more stringent limits on the activation parameter test of the perester thermolysis mechanism,[25] since he felt that anomalies and exceptions to this mechanism test will appear to a significant number. Pryor suggested that peresters undergoing thermolysis with $\Delta H^{\ddagger}$ less than 27 kcal/mol *probably* are doing so via the concerted mechanism. Conversely, peresters undergoing thermolysis with $\Delta H^{\ddagger}$ greater than 33 kcal/mol *probably* are doing so via the stepwise mechanism. By Richardson's more relaxed criteria, inspection of the data in Table III leads to the suggestion that **1a**, **1c**, **2a**, and **3a** are undergoing stepwise thermolysis, peresters **2c**, **3c**, **4c**, and **5** are undergoing concerted thermolysis, and peresters **1d** and **4a** are undergoing a

"borderline" or mixture of concerted and stepwise mechanisms.

The Arrhenius E_a values for peresters **2a** and **3a** are 4–5 kcal/mol higher when calculated using rate constants determined between lowest temperatures. These differences in E_a values appear to be significant (outside the error limits). Curved Arrhenius plots could be due to the complicated nature of the stepwise mechanism, or they could be due to the existence of competing mechanisms (concerted vs. stepwise) in the overall decomposition mode. It is interesting that the peresters which appear to be decomposing via the "pure" mechanisms (stepwise for **1a**, concerted for **4a**) do not have curved Arrhenius plots. This tendency was also found for several other peresters. Peresters which undergo thermolysis at rates similar to or slower than **1a** (such as 1-norbornyl[43] and phenyl[44]) have noncurved Arrhenius plots. Noncurved Arrhenius plots are also exhibited for those peresters which undergo thermolysis at rates similar to or faster than **4a** (such as nonstrained bridgehead polycyclics,[43,45] isobutyryl,[46] *exo*- and *endo*-2-norbornyl,[47] *exo*- and *endo*-2-methyl-2-norbornyl,[48] benzyl,[49] and 9-decalyl[50]). A perester which undergoes thermolysis at a rate close to **2a** exhibits a curved Arrhenius plot (α-phenylbutyryl).[51]

The trends in Table III follow our naive ideas regarding substituent effects on energy changes. Thus, as the alicyclic radicals (and the incipient alicyclic radicals in the transition states) are made more stable either by phenyl substitution at the α carbon or by making the ring size larger, the $\Delta H^{\ddagger}$ for the reaction decreases. However, if the thermolysis is occurring by a mixture of mechanisms, or if the seemingly concerted mechanism has some stepwise components (see below), the $\Delta H^{\ddagger}$ and $\Delta S^{\ddagger}$ values are significantly less meaningful. They will be made up of component activation parameters of the contributing reaction steps. Thus, only reactivity–selectivity principle trends involving the $\Delta H^{\ddagger}$ and $\Delta S^{\ddagger}$ of peresters undergoing thermolysis by "truly concerted" mechanisms (i.e., **2c**, **3c**, and **4c**, in this series) are really valid. An additional complication is the well-known difficulty in obtaining precise values for the activation parameters. Rate constants with errors of 1–2% are propagated into enthalpies of activation with 2–4% absolute error. However, the relative error over the spread of values for $\Delta H^{\ddagger}$ for a series of peresters (12.0 kcal in Table III) increases to 6–15%. We believe that Pryor's warnings[25] considering the use of activation parameters as mechanistic probes per se are well founded.

Deuterium Isotope Effects. α deuterium isotope effects and solvent viscosity effects are probably more valid mechanistic tools to bring to bear on the present problem. The results of these tests, summarized in Table VII, suggest that **1a** and **2a** undergo thermolysis primarily by the stepwise mechanism and that **3a** and **4a** undergo thermolysis primarily by the concerted mechanism. The viscosity test strongly suggests the concertedness of the thermolysis mechanism for **2c**, **3c**, **4c**, and **5**. Other evidence for the concerted nature of all 1-aryl substituted cyclobutyl-, cyclopentyl-, and cyclohexylpercarboxylates will be presented in a later paper.[52]

Pryor has pointed out the insensitivity of the deuterium isotope effect test toward small contributions of the stepwise mechanism to an otherwise predominating concerted mechanism for perester thermolysis.[22] He has also pointed out the insensitivity of the viscosity test toward small contributions of the concerted mechanism to an otherwise predominating stepwise mechanism for perester thermolysis. It is interesting that a controversial perester in this regard is *tert*-butyl perisobutyrate (Table VI). The deuterium isotope test and oxygen-18 scrambling test suggest that this perester undergoes thermal decomposition by the concerted pathway. Pryor has measured a solvent viscosity effect on this perester of about the same quantity as we find for **2a** (8–12% rate decrease for

hexadecane vs. octane). He attributes this solvent viscosity effect to a small contribution of the stepwise mechanism to an otherwise predominating concerted mechanism for the thermolysis of *tert*-butyl perisobutyrate. These results are relevant to our series of alicyclic percarboxylates, since the relative rates of thermolysis of *tert*-butyl perisobutyrate and **4a** are so similar (Table VI).

Rüchardt has observed that the α secondary deuterium isotope effects for perester thermolysis are significantly smaller than the analogous isotope effects for diazene thermolysis.[1] This observation was used as additional evidence for his proposing the lack of significant $C(\alpha)$-C(carbonyl) bond breakage in the transition state of perester thermolysis.[1] The α secondary deuterium isotope effect for diazene thermolysis has recently been reanalyzed and found to be significantly lower than previously thought (k_H/k_D = 1.093 per deuterium for thermolysis of 1,1'-diphenylazoethane at 105.3 °C).[44] The larger size for diazene α deuterium effects, as compared to those of peresters, can be explained in terms of the more endothermic nature of diazene thermolysis. This would seem to allow arguments suggesting a substantial reorganization of bonds around the α carbon at the transition state for perester thermolyses for peresters with "large" α deuterium isotope effects (k_H/k_D = 1.05-1.06).

Solvent Viscosity Effects. The solvent viscosity effects measured for **1a–4a** are consistent with the α deuterium isotope effects mentioned above. Those peresters undergoing thermolysis by the stepwise mechanism would be expected to have smaller rates of thermolysis in more viscous solvent, owing to the decrease in k_d (see eq 4 and 6, Scheme 1). Assuming that changes in paraffin solvent viscosity affect *only* k_d, Pryor derived an equation to measure relative magnitudes of some of the individual rate constants in the stepwise decomposition mechanism:[10]

$$\frac{1}{k_0} = \frac{1}{k_1} + \left(\frac{k_c}{A_D k_1}\right)\left(\frac{\eta}{A_V}\right)^{\alpha} \tag{7}$$

where k_1 is the observed overall first-order decomposition rate constant, A_D and A_V are Arrhenius preexponential factors for solute diffusion and self-diffusive flow of solvent, respectively, η is the viscosity of the solvent, and α is a variable fraction, set equal to 0.5 for the calculations discussed below. This quantitative treatment, while attractive for its ease of use, is probably an oversimplification, since Koenig has found evidence that the equilibrium reaction (3) is also affected by solvent viscosity.[23b]

Notwithstanding these problems, we were able to fit eq 7 very well to the measured rate constants for the thermolysis of **1a** at 113.0 °C in three paraffin solvents. The results for **1a** at 113.0 °C and for **1a** and **2a** (both at 102.6 °C, measured only for two paraffin solvents) are shown in Table V. Using the data for **1a** and **2a** from Table V and *assuming* that A_D is approximately the same for geminate radicals derived from **1a** and **2a**, we calculate the following relative relationships:

$$\frac{k_1(\mathbf{2a})}{k_1(\mathbf{1a})} = 2.23 \pm 0.11 \qquad \frac{k_c(\mathbf{2a})}{k_c(\mathbf{1a})} = 0.272 \pm 0.065 \tag{8}$$

This suggests that **2a** undergoes thermolysis faster than **1a** because breakage of the O–O bond occurs *faster* for **2a** and cage recombination occurs *slower* for **2a**.

$$\frac{k_1(\mathbf{1a}, 113.0\ °C)}{k_1(\mathbf{1a}, 102.6\ °C)} = 3.33 \pm 0.23 \tag{9}$$

$$\frac{k_c(\mathbf{1a}, 113.0\ °C)}{k_c(\mathbf{1a}, 102.6\ °C)} = 0.75 \pm 0.16$$

Since the overall rate of decomposition of **1a** at 113.0 °C is 3.62 times faster than the rate of decomposition of **1a** at 102.6 °C, this suggests that this difference can be accounted for mainly
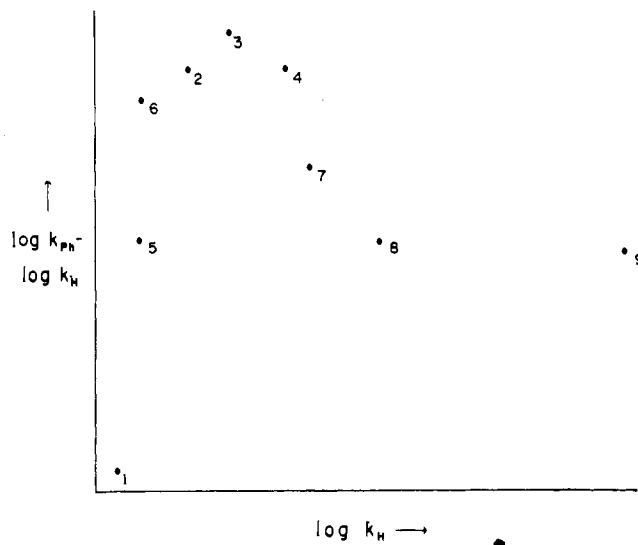

Figure 1. Reactivity–selectivity plot for perester thermolysis. Data and numbering scheme for pairs of peresters from Table XII.

by the temperature effect on breaking the O–O bond. The geminate recombination process is relatively temperature insensitive.

An attempt was made to fit the rate constants for the thermolysis of **1a** at 113.0 °C in the three paraffin solvents to another solvent effect parameter. The Hildebrand solubility parameter (δ) measures the total molecular cohesion per mL of solvent.[54] If δ is linearly related to the logarithm of the rate constant for thermolysis in that solvent, the main solvent effect would be the influence of solvent on the energy necessary for the reactant to change the solvent cavity in going from ground state to transition state.[55] Since we find a curved plot of log k vs. δ for the thermolysis of **1a** in the admittedly limited number of three paraffin solvents, this suggests that differences in energy for changes of solvent cavity for step 3 of Scheme I are not important.

Reactivity–Selectivity Principle. The reactivity–selectivity principle has been used to discover linear free energy effects for molecules decomposing by similar mechanisms.[56] Although a linear log–log plot is not proof of similarities in transition states for the two series of reactions, a nonlinear log–log plot probably suggests dissimilar transition states (different mechanisms, nonlinear variation of reaction coordinates with structure variation, or different effects of structure variation on $\Delta H^{\ddagger}$ and $\Delta S^{\ddagger}$).[57] We attempted a reactivity–selectivity plot, using the data in Table XI and using Giese's criterion that a reactivity–selectivity relationship would show up as a negatively sloping log ($k(Ph)/k(H)$) vs. log $k(H)$ plot.[56] This plot is shown in Figure 1.

The slope of the log–log plot changes from positive to negative at approximately the values for the rate constant of the thermolysis of **3a**. This suggests a changeover in mechanism at this point on the log–log plots. Thus perester pairs whose X = H member undergoes thermolysis faster than **3a** may exhibit the same mechanism of decomposition (presumably *concerted*) for both the X = H and X = Ph pairs. Perester pairs whose X = H member undergoes thermolysis more slowly than **3a** may exhibit different mechanisms of decomposition for the X = H member (presumably *stepwise*) than for the X = Ph member (presumably *concerted*, except for **1c**). This result is consistent with the evidence from the activation parameter, deuterium isotope effect, solvent viscosity effect, and Arrhenius plot investigations cited earlier.

Discrete vs. Merged Mechanisms. The question arises as to whether the "borderline" peresters (**2a** and **3a**) undergo thermolysis by two competing mechanisms (stepwise and

Scheme II

$k_c \geqslant k_d$ and $k_c \geqslant k_2$

$k_c \leqslant k_d$ and $k_c < k_2$
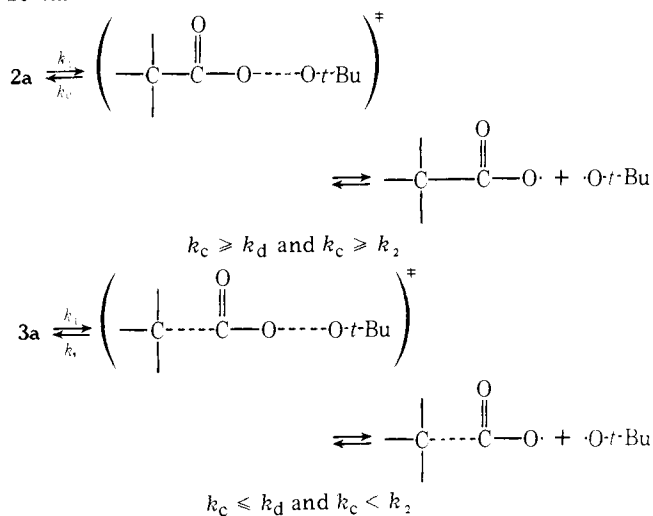
concerted) or by a "merged" mechanism. The "merged" mechanism would have intermediate acyloxy radicals with stretched $C(\alpha)$–C(carbonyl) bonds in the transition states for formation of the acyloxy radicals (Scheme II).

Arguments based on the "reacting bond rule", similar to those made for S_N-type reactions[60] and eliminations,[61] could be made in the case of the thermolysis of peresters. A recent extended discussion of structural changes on transition states suggests that these arguments may prove valuable for analyzing many organic reactions.[62] We lean toward the "merged" mechanism proposal for the thermolysis of peresters, based tenuously on the data at hand (for example, the successful correlation of eq 7 for the thermolysis of **1a**). We are, however, aware of results of molecular orbital calculations which suggest that peresters decompose thermally by *three* discrete mechanisms, one (stepwise) giving π carboxy intermediates, another (quasi-concerted) giving short-lived σ carboxy intermediates, and the third a true concerted mechanism.[63] This issue can perhaps only be resolved by high-quality molecular orbital calculations.

Structural Effects of Peresters and Their Rates of Thermolysis. The question remains concerning the validity of Rüchardt's picture of the mechanism of perester thermolysis (discussed above). Ample evidence exists to support Rüchardt's claim that most perester thermolyses are driven primarily by polar effects. Independent evidence suggests that cyclohexyl radicals are nucleophilic[64] and that the cyclopropyl group is rather strongly inductively electron withdrawing.[65] Evidence regarding the polar characteristics of the cyclopropyl radical is conflicting. Studies suggesting that the cyclopropyl radical has very little polar character (and thus is more electrophilic than the cyclohexyl radical)[66] contrast with studies suggesting that the cyclopropyl radical is indeed nucleophilic.[67] Recent evidence suggests that there are no significant polar effects for formation of bridgehead radicals from either perester thermolysis or tin hydride reduction of bridgehead halides.[68] Fort proposes that the rates of formation of the bridgehead radicals are determined by the relative stabilities of the radicals (affected by ring strain).

Rüchardt asserts that, for the thermolysis of alicyclic peresters, relief (or increase) of strain is accomplished early at the transition state and is not a big factor in determining relative rates of thermolysis of these peresters. For acyclic peresters relief of ground-state strain (B-strain) is a small but measurable factor in influencing rates of thermolysis. Experiments by Tidwell,[69] Timberlake,[70] and Friedman,[71] in which the size of the alkyl groups attached to the α position of peresters was varied, suggest that relief of B-strain does influence the rates

of thermolysis of peresters. This influence, however, seems to be smaller than the same influence on rates of thermolyses of diazenes.[70,72,73] The proposal exists, of course, that radical *stability* is determined more by steric factors than by electronic factors.[74]

We believe that the thermolysis rates of alicyclic peresters **1a–5** (i.e., the 1-H series) are determined by a complicated combination of ring strain effects and polar effects. Steric effects (B-strain) are probably not important for this series. This conclusion is in agreement with conclusions made by Fort as to the mechanism of thermolysis of peresters.[15,68] For the 1-H alicyclic series, the relative rates of "pure concerted" thermolysis mechanism, after subtracting out the contribution from the stepwise mechanism, would be in the order (fastest to slowest)

$$5 > 4a > 3a \gg 2a \gg 1a$$
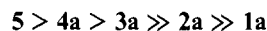
We doubt that the logarithms of the rates of these "pure concerted" mechanisms (hypothetical for **2a** and **1a**) would correlate well with ^{13}C–H coupling constants or other measurements of purely polar effects.[1]

We have reservations, moreover, about using the thermolysis of diazenes as a better model for measuring the "correct" ring strain effects in alicyclic radical forming reactions. Until the controversy of one-bond vs. two-bond mechanism for diazene thermolysis is resolved[75] and until the contribution of ground-state stabilities of the trans diazenes to the overall rates of diazene decomposition is understood more[76] (especially in the cyclic diazene series), the thermolysis of bisalicyclic diazenes seems to us to be a compromised model for the formation of cyclic radicals. Indeed, if one compares the rates of "pure concerted" thermolysis of alicyclic peresters to the rates of thermolysis of bisalicyclic diazenes, the only anomalous perester is **4a**. Perhaps this anomaly could be rationalized by invoking contributions of the nucleophilicity of the cyclohexyl ring (stabilizing the transition state by polar effects) offsetting the ring strain appearing at the incipient cyclohexyl radical at the transition state.

It is possible that the 1-H alicyclic perester series (**1a–5**) is a better model series for measuring ring strain effects than the 1-CH_3- or 1-phenyl alicyclic series (**1c–4c**). The resonance stabilization of the developing radical by alkyl or aryl substituents at the α position of these peresters may overwhelm any ring strain effects. This is suggested by the small ring size effects on rates for the "pure concerted" thermolysis of **2c–4c** (Table III).

Radical-Induced Decomposition. We attempted to investigate more carefully the radical-induced mode of decomposition for perester series **1a–4a**. The larger first-order rate constants and curved log (perester) vs. time plots, illustrated in Table VIII for **4a**, were consistent phenomena for the thermolysis of **1a–4a** under conditions of no added radical scavenger and high initial perester concentration. We attempted to determine the order n of the higher order term (eq 10) for the rate expression by the method of drawing tangents (i.e., differentiating) to the concentration of perester vs. time curves for the thermolysis of **1a–4a** under these conditions:

$$\text{rate} = k_0(\text{perester}) + k'(\text{perester})^n \qquad (10)$$

This method, only partly successful, leads to the conclusion that $n = 1.7 \pm 0.2$ for **4a** and $n = 1.3 \pm 0.2$ for **1a**, **2a**, and **3a**.

Attempts have been made in the past to extract quantitative estimates of the induced-decomposition rate constant for peroxide thermolysis.[41,77] These efforts were only modestly successful, owing to the large scatter in kinetic data points and generally poorly reproducible kinetic results. We attempted to use the Bartlett–Nozaki method to analyze our results, with little success.[77] Recently, Huyser used a computer fit technique

Table IX. Three-Halves Order Rate Constants and Deuterium Isotope Effects for Thermal Decomposition of Peresters in 2,2,4-Trimethylpentane Solvent

perester	temp, °C	$k' \times 10^4$ [a]	k'_H/k'_D [b]
1a	113.0	0.23 ± 0.05	2.2 ± 0.6
1a	102.6	0.06 ± 0.01	4.4 ± 1.6
2a	113.0	1.22 ± 0.33	1.7 ± 0.9
2a	102.6	0.36 ± 0.19	2.6 ± 2.0
3a	102.6	0.41 ± 0.08	1.1 ± 0.8
3a	92.9	0.12 ± 0.03	3.0 ± 1.5
4a	113.0	6.08 ± 0.02	2.0 ± 0.1
4a	102.6	1.64 ± 0.12	1.8 ± 0.2
4a	92.9	0.57 ± 0.03	1.8 ± 0.2
4a	82.2	0.15 ± 0.01	1.6 ± 0.1

[a] Calculated from eq 11. Each value for **1a–4a** and **1b–4b** represents an average of three to four separate kinetic runs. Errors are standard deviations. [b] Errors are propagated from the standard deviations of the separate average rate constants.

to calculate the overall kinetic order for the induced decomposition of isopropyl *tert*-butyl peroxide.[78] We tried a somewhat different approach: iterative calculation of the integrated rate expression. We assumed an exponent of 1.5 in the second term of eq 10. Integrating eq 11 led to eq 12.

$$\frac{-d(\text{perester})}{dt} = k_0(\text{perester}) + k'(\text{perester})^{1.5} \quad (11)$$

$$k_0 t = \ln(A_t) - 2\ln(MA_t^{1/2} + k_0) \quad (12)$$

where A_t = absorbance due to perester carbonyl stretching peaks at time t, $M = k'\epsilon^{-1/2}$, where ϵ = molar absorptivity of the perester carbonyl chromophore. A computer program was written which used the known values of k_0 (from Table I) and measured values of ϵ and A_t. The program varied k' through many possible values, and the value of k' which gave a slope equal to k_0 on the left of eq 12 was chosen as the "correct" value. The correlation coefficients for the plots using the "correct" k' value were larger than 0.999.

The results of these calculations are presented in Table IX. The errors from the averages (standard deviations) are substantial, yet certain tentative conclusions from these data can be drawn. The induced rate constants (k') increase as the size of the ring increases, in line with the results of hydrogen-atom abstractions of cyclanes.[8] The suggestion that the actual induced mode of decomposition of **1a–4a** may be due to free-radical attack on the α hydrogen is reinforced by the deuterium isotope effects for k' (fourth column of Table IX). The ratio k'_H/k'_D should be a measure of k_P^H/k_P^D (the chain propagation rate constants).[20] The values in Table IX for the deuterium isotope effects are large enough to be considered as possible primary effects.[79,80] Radical attack on α hydrogens of peresters has already been proposed, and the resulting radicals appear to lead to α-lactones.[50,81,82] Since we do not know which radical is doing the attacking, although it is probable that it is an alkoxy radical, owing to the presence of oxygen in the reaction tubes, we did not analyze the magnitude of the primary deuterium effects along the elegant lines taken by Pryor.[83] The suggestion remains, however, that radical-induced decomposition of **1a–4a** occurs significantly by attack at the α hydrogen. Radical attack at the O–O bond cannot be ruled out as a small contributor to the overall induced decomposition mode, however.

Experimental Section

Spectral Analyses. Analytical NMR spectra for all compounds were measured on a Varian T-60 spectrophotometer. Infrared spectra and kinetic measurements were recorded on either a Beckman IR-33 or a Beckman Acculab spectrophotometer, using liquid-phase NaCl cells. Beer's law behavior for the carbonyl stretching peak of each perester

Table X. Summary of Proposed Mechanisms for Alicyclic Peresters

perester	mechanism	perester	mechanism
1a, (1b)	stepwise	3a (3b)	primarily concerted
1c	stepwise	3c	concerted
1d	stepwise	4a (4b)	concerted
2a (2b)	primarily stepwise	4c	concerted
2c	concerted	5	concerted

Table XI. Logarithms of Some Rate Constants for Thermolysis of Peresters

perester	R, in RCO_3-t-Bu	log k (X = Ph) [a]	log k (X = H) [a]
1		0.427[b]	0.234[b]
2		3.326[b]	0.684[b]
3		3.823[b]	0.948[b]
4		3.964[b]	1.307[b]
5	X-CH$_2$-	1.903[c]	0.357[d]
6	alkyl-CHX-	2.832[c]	0.380[e]
7	(CH$_3$)$_2$CX-	3.480[c]	1.455[f]
8	Ph-CHX-	3.464[f]	1.903[c]
9	Ph$_2$-CX-	4.949[g]	3.464[f]

[a] Rate constants at 102.6 °C, calculated from activation parameters for all peresters except **1a**, **1c**, **2a**, **3a**, and **4a**. [b] This work. [c] Reference 21a. [d] Reference 13. [e] Reference 58. [f] Reference 50. [g] Reference 59.

was established for both spectrophotometers. Spectral characteristics of the peresters corresponded exactly to those reported by Rüchardt.[2,16]

Deuterium Analyses. Estimates of the percent deuterium incorporated into the peresters **1a–4a** and their synthetic precursors were made on the basis of integrations of relevant peaks in the NMR and by mass spectral analysis of the carboxylic acids (Du Pont Model 21-490). The α protons of the alicyclic carboxylic acids, acid chlorides, and peresters appear at chemical shifts downfield from the rest of the alicyclic ring protons. On the 60-MHz instrument the separations of the upfield tail of the α proton peak and the downfield tail of the other alicyclic proton peaks were at least 0.3 δ units (more for the acid chlorides) for all the carboxylic acids and peresters except cyclohexanecarboxylic acid and **4a**. The *tert*-butyl peak for **1a** did overlap the α proton peak slightly. The 100-MHz spectra of **4a** and **4b** were taken, with resulting better separation of the α proton peak from the other ring protons.[84] In all cases the calculations of percent deuterium incorporated into α positions were in close agreement from the NMR spectra of the carboxylic acids, acid chlorides, and peresters and from the mass spectra of the carboxylic acids (to within 5%). The percent incorporation of deuterium for **1b–4b** is given below.

perester (and precursor acid and acid chloride)	% D in α position
1b	>95
2b	85
3b	>95
4b	60

The recycled deuterium oxide used to prepare the deuterated precursor to **4b** was analyzed by NMR to be only 80% deuterated.

Kinetics. The disappearance of each perester's carbonyl stretching bond at 1770–1780 cm^{-1} was followed by infrared. Each reaction point of a kinetic run was on an individual reaction tube partially filled with the perester–styrene–solvent solution. The kinetic reaction tubes were prepared from 8 mm o.d. uniform diameter glass tubes, approximately 10 cm in length. The tubes were sealed at one end with a torch, rinsed in distilled water, and dried in a drying oven. Changing

Table XII

carboxylic acid chloride	boiling range, °C (Torr)	
cyclopropanecarbonyl chloride (d_0 and d_1)	27–28 (40)	lit. 119 (760) ref 86, p 224
cyclobutanecarbonyl chloride (d_0 and d_1)	134–136 (757)	lit. 60 (50) ref 86, p 211
cyclopentanecarbonyl chloride (d_0 and d_1)	75–77 (50)	lit. 72–74 (50) ref 87
cyclohexanecarbonyl chloride (d_0 and d_1)	95–97 (50)	lit. 184 (760) ref 86, p 215
cycloheptanecarbonyl chloride	91–95 (30)	lit. 84–86 (14) ref 16
1-methylcyclopropanecarbonyl chloride	128–131 (755)	lit. 128–129 (atm) ref 88
1-phenylcyclopropanecarbonyl chloride	119–121 (30)	lit. 76 (0.4) ref 2
1-phenylcyclobutanecarbonyl chloride	138–140 (30)	lit. 108 (1) ref 2
1-phenylcyclopentanecarbonyl chloride	160–163 (35)	lit. 140 (1) ref 2
1-phenylcyclohexanecarbonyl chloride	124–127 (2)	lit. 107 (0.1) ref 2

the type of glass used in the reaction tubes (Pyrex vs. "soft glass") and rinsing the tubes with organic solvents prior to the water rinse had no effect on the rates of reaction.

After a reaction tube was partially filled with approximately 0.40 mL of solution, the other end of the tube was sealed by torch. The tubes were stored in a freezer (-10 °C) until the kinetic runs were performed. A kinetic run was obtained by placing the filled tubes in a constant temperature (± 0.05 °C, using corrected thermometer) oil bath. The tubes were allowed to equilibrate in the bath for 2 min, before T_0 was established. At timed intervals, tubes were removed from the bath, quickly placed in an ice-water bath to "quench" the perester thermolysis, dried, labeled, and stored in the freezer. Several kinetic runs, for several different compounds, could be done simultaneously using this procedure.

A kinetic run consisted of from 12 to 25 reaction tube points. The analysis procedure consisted of breaking open each reaction tube, withdrawing the contents via a clean Pasteur pipet, filling a 1.0-mm width sodium chloride infrared cell with the solution, and scanning the spectrophotometer at constant wavelength. Readings were recorded in percent transmittance (to the nearest 0.1%) and later converted to absorbances. Care was taken to ensure that the thermal history of each tube in a particular run was similar before and after the kinetic experiment. Infinity point tubes were prepared by either allowing the thermolysis to proceed on a few tubes for at least 10 half-lives or by accelerating the thermolysis by placing some tubes in an oven set at higher temperatures than those of the kinetics. No difference between the infinity point readings for the two methods could be detected.

The values of the rate constants were determined by a linear regression analysis (linear least squares). The standard errors of the slopes were calculated from the square root of the difference between variance of ordinate (ln $(A_t - A_\infty)$) and abscissa (time). Average values of rate constants and all other values expressed in this paper are given with standard deviations ($n - 1$).

The values of the rate constants are, of course, heavily dependent on the transmittance values for the infinity points. We could detect no curvature in the individual first-order kinetic plots. To further test the reliability of our infinity points, we subjected many of the kinetic runs to the Guggenheim analysis. The first-order rate constants calculated by this procedure were the same as those calculated using the measured absorbances for the infinity points in all cases for the low perester concentration plus added styrene runs (within experimental error). The Guggenheim-calculated absorbances for the infinity points were the same as the measured values. No curvature in the Guggenheim plots could be detected.

Solvents and Materials. All hydrocarbon solvents (except squalane) used for the reaction kinetic solutions were distilled prior to use, with the forerun being discarded. Reagent-grade hydrocarbon solvents (isooctane, dodecane, hexadecane, and squalane) were purchased from Aldrich Chemical and from Eastman Organic Chemicals.

tert-Butyl hydroperoxide (Aldrich) was distilled prior to use at 30 mm (bp 35 °C). A forerun and sizable amount of distillation pot residue were discarded. Thionyl chloride (Baker and Pfaltz and Bauer) was distilled immediately before use in the preparation of acid chlorides. Deuterium oxide (>99.8% D, Aldrich or Stohler Isotope Chemicals) was used as received.

Materials. The precursor organic chemicals for the synthesis of the peresters in this study were all purchased from Aldrich Chemical Co. and used without further purification. These are cyclopropane-, cyclobutane-, cyclopentane-, cyclohexane-, and cycloheptanecarboxylic acids, methyl cyclopropyl ketone, cyclobutane-1,1-dicarboxylic acid,

diethyl malonate, 1,4-dibromobutane, methallyl alcohol, 1-phenylcycloalkanecarboxylic acids, methylene iodide, and methyl iodide. Zinc–copper couple was purchased from Alfa Inorganics.

General Methods. Peresters were synthesized by the method previously described.[21a,85] Peresters were purified by column chromatography through silica gel or alumina, using diethyl ether eluant or by recrystallization from 2,2,4-trimethylpentane. The peresters were pumped free of solvent by high-vacuum pump. Yields of peresters were typically 50–80% from the acid chlorides. Purities were established by NMR and infrared spectra.

Carboxylic acid chlorides were prepared from the carboxylic acids by refluxing a 3 M solution of acid in dry benzene with 3–4 equiv of thionyl chloride for 5–10 h. The excess thionyl chloride and benzene were removed by distillation at atmospheric pressure. The acid chlorides were then distilled under reduced or atmospheric pressure (Table XII).

Deuterated Alicyclic Carboxylic Acids. The elaborate synthetic schemes outlined below were necessitated by our inability to accomplish the direct deuterium exchange of the acids under highly basic conditions at elevated temperatures (sealed tube reactions).[89] We experienced extensive decomposition of the carboxylic acids and only modest deuterium exchange at the 1 position under these conditions.
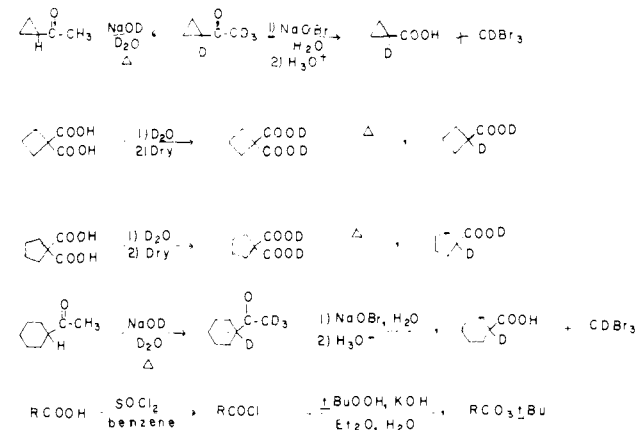
Methyl Cyclopropyl Ketone-$\alpha,\alpha,\alpha,\alpha'$-$d_4$. The α protons of cyclopropyl methyl ketone (0.20 mol) were exchanged by refluxing in basic deuterium oxide. Yield of d_4 ketone was 9.0 g (0.102 mol 51% yield), NMR (CCl$_4$) δ 0.73–0.97 (m).

Cyclopropanecarboxylic Acid-α-d_1. The bromoform reaction on the ketone was performed according to the method reported by Vogel.[90] From 0.101 mol of methyl cyclopropyl ketone-d_4 was obtained 8.0 g of cyclopropanecarboxylic acid-α-d_1 (0.084 mol, 83% yield): NMR (CCl$_4$) δ 0.97–1.37 (4 H) and 9.50 (1 H).

1,1-Cyclobutanedicarboxylic Acid-O,O'-d_2. 1,1-Cyclobutanedicarboxylic acid (0.100 mol, mp 160–162 °C) was added to 100 mL (4.99 mol) of deuterium oxide and stirred at ambient for 2 h: yield 14.50 g of cyclobutanedicarboxylic acid-d_2 (0.100 mol, 100% yield); mp 157–158 °C (lit.[9] 157 °C); NMR (CCl$_4$) δ 0.80 (m, 2 H) and 1.56 (m, 4 H).

Cyclobutanecarboxylic Acid-α,O-d_2. The dibasic acid (14.4 g, 0.0985 mol) was placed in a dried 250-mL round-bottomed flask, with condenser and drying tube. The flask was placed in an oil bath, and the bath was maintained between 160 and 170 °C. Heating was continued until evolution of gas (CO$_2$) ceased (5 h). The product was

distilled at atmospheric pressure, and the fraction between 186.0 and 189.5 °C (lit.[96] 195 °C (760 mm) was collected; yield 10.0 g of monocarboxylic acid (0.0979 mol, 99.4% yield); NMR (CCl₄) δ 1.37–2.05 (m, 6 H) and 2.53–3.00 (m, 0.16 H).

1,1-Cyclopentanedicarboxylic Acid. The dibasic acid was prepared according to the method of Haworth and Perkin.[92] Diethyl malonate (0.1875 mol), 1.4-dibromobutane (0.1875 mol) and sodium (0.375 g-atom) in 175 ml of absolute ethanol were used. The dibasic acid was prepared by saponification of the diester by refluxing potassium hydroxide (0.658 mol) in absolute ethanol (175 mL). The dibasic acid was recrystallized from hot water, using Norite. Yield of dried 1,1-cyclopentanedicarboxylic acid was 9.50 g (0.060 mol, 32% yield): mp 199–200 °C (lit.[91] 183–184 °C); NMR (CCl₄) δ 0.90 and 1.40 (m, 8 H) and 7.70 (s, 2 H).

Cyclopentanecarboxylic Acid-α,O-d₂. Cyclopentane-1,1-dicarboxylic acid was converted to cyclopentanecarboxylic acid-α,O-d₂ by the same procedure described above for the synthesis of cyclobutanecarboxylic acid-α-O-d₂. A yield of 65.7% of the monocarboxylic acid was obtained after distillation at 6 Torr (material collected at 139–141 °C) (lit.[97] 216 °C (760 mm), NMR (CCl₄) δ 1.30–2.20 (m).

Methyl Cyclohexyl Ketone. Methyl cyclohexyl ketone was prepared from the addition of methylmagnesium iodide (0.150 mol) to cyclohexanecarbonyl chloride (0.140 mol) in diethyl ether. Material distilling at 58–70 °C (20–30 Torr) (lit.[93] 64–65.5 °C (12 Torr)) was collected as the desired product: yield 7.95 g (0.0631 mol, 45.1%); NMR (CCl₄) δ 0.97–2.50 (m) and 2.03 (s).

Cyclohexyl Methyl Ketone-α,α,α,α'-d₄. Cyclohexyl methyl ketone-d₄ was prepared by the same method described above for the preparation of cyclopropyl methyl ketone-d₄. The ketone was not distilled after removal of the diethyl ether, NMR (CCl₄) δ 0.97–2.30 (m).

Cyclohexanecarboxylic Acid-α-d₁. Cyclohexanecarboxylic acid-α-d₁ was prepared from the d₄ ketone via the bromoform reaction. The same procedure was used as described above for the preparation of cyclopropanecarboxylic acid-d₁, except that a small amount of 1,4-dioxane was added to the reaction mixture so that a one-phase reaction solution could be maintained. After evaporation of the ether from the extractions, a white solid resulted: mp 29–31 °C (lit.[98] 30–32 °C); NMR (CCl₄ 60 MHz) δ 0.93–2.23 (m, 10 H), 2.23–2.40 (m, 0.4), and 11.97 (s, H); NMR (CDCl₃, 100 MHz) δ 1.10–2.20 (m, 10 H), 2.20–2.50 (m, 0.39 H), and 11.32 (s, 1 H).

1-Methylcyclopropylcarbinol. A Simmons–Smith carbenoid addition[94] to the double bond of methallyl alcohol was accomplished in good yield. Methylene iodide (308 g, 1.15 mol), iodine (1.0 g), zinc-copper couple (99 g), and 750 mL of anhydrous diethyl ether were placed in a 3-L three-necked flask equipped with condenser, addition funnel, and thermometer. The mixture was stirred magnetically and heated to a constant 40 °C. Methallyl alcohol (36.0 g, 0.50 mol) was slowly added. The reaction mixture was stirred for an additional 30 min after the addition was completed. Saturated aqueous ammonium chloride was added (slowly at first) until in excess. The ether fraction was separated, and the aqueous fraction was washed with more diethyl ether. The combined ether fractions were extracted with saturated aqueous ammonium chloride, saturated aqueous potassium carbonate, and saturated aqueous sodium chloride. The ether layer was dried over anhydrous sodium sulfate, and the ether was removed under reduced pressure. The residue was distilled, and 1-methylcyclopropylcarbinol was collected at 98–102 °C (atmospheric pressure) (lit.[95] 125.8–126.3 °C (739 mm)). Yield was 32.64 g (0.379 mol, 75.8%). NMR (CCl₄): δ 0.60 (m, 4 H), 1.15 (s, 3 H), 1.80 (s, 1 H), and 3.30 (s, 2 H).

1-Methylcyclopropanecarboxylic Acid. Into a 1-L round-bottomed flask were placed 1-methylcyclopropylcarbinol (20 g, 0.232 mol), potassium permanganate (48.8 g, 0.309 mol), and 400 mL of 10% aqueous potassium hydroxide. The magnetically stirred solution was kept at 45 °C or below for 20 min, and then the reaction solution was heated to reflux for 30 min. Enough sodium bisulfite was added to the cooled solution to reduce the excess potassium permanganate to manganese dioxide. The manganese dioxide was filtered by gravity, and the filtrate was extracted with diethyl ether to remove neutral organic impurities. The aqueous fraction was acidified with 6 N hydrochloric acid and extracted with diethyl ether. The ether layer was dried over anhydrous sodium sulfate and filtered, and the ether was removed under reduced pressure: yield 5.0 g (0.050 mol, 21.5% yield) of 1-methylcyclopropanecarboxylic acid; mp 31–32 °C (lit.[95] 32.4–34.3 °C); NMR (CCl₄) δ 0.57–0.90 (m, 2 H), 1.20–1.50 (m)

and 1.30 (s) (5 H), and 12.42 (s, 1 H); infrared broad peak at 3000 cm⁻¹ (OH), strong peak at 1700 cm⁻¹ (carbonyl), peak at 1028 cm⁻¹ (cyclopropyl CH₂).

References and Notes

(1) Rüchardt, C. *Angew. Chem., Int. Ed. Engl.* **1970**, *9*, 830.
(2) Bonnekessel, J.; Rüchardt, C. *Chem. Ber.* **1973**, *106*, 2890.
(3) Rüchardt, C.; Beckhaus, H. D.; Bonnekessel, J.; Bock, H.; Dempewolf, E.; Groeger, F. A.; Golzke, V.; Hamprecht, G.; Herwig, K.; Hinz, J.; Lorenz, P.; Mayer-Ruthardt, I.; Muller, J.; Oberlinner, A.; Schacht, E. "23rd International Congress of Pure and Applied Chemistry, Special Lectures", Vol. 4, Butterworths, London, 1971, p. 223.
(4) Trahanovsky, W. S.; Fox, N. S. *J. Am. Chem. Soc.* **1974**, *96*, 7968.
(5) (a) Heine, H. G.; Hartmann, W.; Kory, D. R.; Magyar, J. G.; Hoyle, C. K.; McVey, J. K.; Lewis, F. D. *J. Org. Chem.* **1974** *39*, 691. (b) Lewis, F. D.; Johnson, R. W. *J. Am. Chem. Soc.* **1972**, *94*, 8914.
(6) Britten-Kelly, M. R.; Goosen, A.; Scheffer, A. *J. S. Afr. Chem. Inst.* **1975**, *28*, 224.
(7) Hart, H.; Wyman, D. P. *J. Am. Chem. Soc.* **1959**, *81*, 4891.
(8) Walling, C.; Fredricks, P. S. *J. Am. Chem. Soc.* **1962**, *84*, 3326.
(9) Klug, J. H. *Diss. Abstr. Int. B* **1971**, *31*, 7188.
(10) Pryor, W. A.; Smith, K. *J. Am. Chem. Soc.* **1970**, *92*, 5403.
(11) Koenig, T.; Huntington, J. *G. J. Am. Chem. Soc.* **1974**, *96*, 592.
(12) Koenig, T. In "Free Radicals", Vol. 1; Kochi, J. K., Ed.; Wiley: New York, N.Y., 1973; p 135.
(13) Reference 12, p 131.
(14) Lorand, J. P.; Chodroff, S. D.; Wallace, R. W. *J. Am. Chem. Soc.* **1968**, *90*, 5266.
(15) Fort, R. C.; Franklin, R. E. *J. Am. Chem. Soc.* **1968**, *90*, 5267.
(16) Lorenz, P.; Rüchardt, C.; Schacht, E. *Chem. Ber.* **1971**, *104*, 3429.
(17) Reference 12, pp 120–136.
(18) Criegee, R. *Chem. Ber.* **1944**, *77*, 722.
(19) Reference 12, p 114.
(20) Swain, C. G.; Stockmayer, W. H.; Clarke, J. T. *J. Am. Chem. Soc.* **1950**, *72*, 5426.
(21) (a) Koenig, T.; Wolf, R. *J. Am. Chem. Soc.* **1969**, *91*, 2574. (b) Koenig, T.; Huntington, J.; Cruthoff, R. *J. Am. Chem. Soc.* **1970**, *92*, 5413.
(22) Pryor, W. A.; Morkved, E. H.; Bickley, H. T. *J. Org. Chem.* **1972**, *37*, 1999.
(23) (a) Koenig, T. W.; Fischer, H. In ref 12, p 157. (b) Koenig, T. W. "Symposium on the Chemistry of Free Radicals", 174th National Meeting of the American Chemical Society, Chicago, Ill., Aug. 1977. "ACS Symposium Series 69", American Chemical Society: Washington D.C., 1978; p 134. We thank Professor Koenig for a preprint of this article.
(24) Bartlett, P. D.; Hiatt, R. C. *J. Am. Chem. Soc.* **1958**, *80*, 1398.
(25) Pryor, W. A.; Smith, K. *Int. J. Chem. Kinet.* **1971**, *3*, 387.
(26) Richardson, W. H.; Koskinen, W. C. *J. Org. Chem.* **1976**, *41*, 3182.
(27) (a) Neuman, R. C., Jr.; Behar, J. V. *J. Am. Chem. Soc.* **1969**, *91*, 6024. (b) Neuman, R. C., Jr.; Pankrantz, R. P. *ibid.* **1973**, *95*, 8372.
(28) Reference 23a, p 159.
(29) Martin, J. C.; Taylor, J. W.; Drew, E. H. *J. Am. Chem. Soc.* **1967**, *89*, 129.
(30) Walborsky, H. M.; Collins, P. C. *J. Org. Chem.* **1976**, *41*, 940.
(31) Ishihara, T.; Hayashi, K.; Ando, T.; Yamanaka, H. *J. Org. Chem.* **1975**, *40*, 3264.
(32) Koenig, T.; Hoobler, J. A.; Mabey, W. R. *J. Am. Chem. Soc.* **1972**, *94*, 2514.
(34) Creary, X. *J. Am. Chem. Soc.* **1976**, *98*, 6608.
(35) (a) Streitwieser, A., Jr.; Caldwell, R. A.; Young, W. R. *J. Am. Chem. Soc.* **1969**, *91*, 529. (b) Streitwieser, A., Jr.; Young, W. R.; Caldwell, R. A. *ibid.* **1969**, *91*, 527.
(36) Hinz, J.; Rüchardt, C. *Justus Liebigs Ann. Chem.* **1972**, *94*, 765.
(37) Kirchen, R. P.; Sorensen, T. S. *J. Am. Chem. Soc.* **1977**, *99*, 6687.
(38) Wood, D. W.; Williams, L. F.; Sprecher, R. F.; Lathan, W. A. *J. Am. Chem. Soc.* **1972**, *94*, 6241.
(39) Koenig, T.; Balle, T.; Chang, J. C. *Spectrosc. Lett.* **1976**, *9*, 755.
(40) Bakuzis, P.; Kochi, J. K.; Krusic, P. J. *J. Am. Chem. Soc.* **1970**, *92*, 1434.
(41) Lamb, R. C.; Vestal, L. L.; Cipau, G. R.; Debnath, S. *J. Org. Chem.* **1974**, *39*, 2096.
(42) Schuster, G. B. *J. Am. Chem. Soc.* **1977**, *99*, 6107.
(43) (a) Fort, R. C.; Franklin, R. E. *J. Am. Chem. Soc.* **1968**, *90*, 5267. (b) Humphrey, L. B.; Hodgson, B.; Pincock, R. E. *Can. J. Chem.* **1968**, *46*, 3099.
(44) Blomquist, A. T.; Ferris, A. F. *J. Am. Chem. Soc.* **1951**, *73*, 3408.
(45) Lorand, J. P.; Chodroff, S. D.; Wallace, R. W. *J. Am. Chem. Soc.* **1968**, *90*, 5266.
(46) Bartlett, P. D.; Gortler, L. B. *J. Am. Chem. Soc.* **1963**, *85*, 1864.
(47) Bartlett, P. D.; McBride, M. *J. Am. Chem. Soc.* **1965**, *87*, 1727.
(48) Schindel, W. G.; Pincock, R. E. *J. Org. Chem.* **1970**, *35*, 1789.
(49) Bartlett, P. D.; Rüchardt, C. *J. Am. Chem. Soc.* **1960**, *82*, 1756.
(50) Bartlett, P. D.; Pincock, R. E.; Rolston, J. H.; Schindel, W. G.; Singer, L. A. *J. Am. Chem. Soc.* **1965**, *87*, 2590.
(51) Martin, M. M. *J. Am. Chem. Soc.* **1962**, *84*, 1986.

(52) Wolf, R. A. Unpublished results.
(53) Scheppele, S. E.; Grizzle, P. L.; Miller, D. W. *J. Am. Chem. Soc.* **1975,** *97,* 6165.
(54) Hildebrand, J. H.; Prausnitz, J. M.; Scott, R. L. "Regular and Related Solutions", Van Nostrand-Reinhold: Princeton, N.J., 1970; pp 207–215.
(55) Sanderson, J. R.; Story, P. R. *J. Org. Chem.* **1974,** *39,* 3463.
(56) Giese, B. *Angew. Chem., Int. Ed. Engl.* **1977,** *16,* 125.
(57) Pryor, W. A.; Smith, K. *J. Am. Chem. Soc.* **1970,** *92,* 2731.
(58) Trachtman, M.; Miller, J. G. *J. Am. Chem. Soc.* **1962,** *84,* 4928.
(59) Bartlett, P. D.; Lorand, J. P. *J. Am. Chem. Soc.* **1966,** *88,* 3294.
(60) Thornton, E. R. *J. Am. Chem. Soc.* **1967,** *89,* 2915.
(61) More O'Ferrall, R. A. *J. Chem. Soc. B* **1970,** 274.
(62) Jencks, D. A.; Jencks, W. P. *J. Am. Chem. Soc.* **1977,** *99,* 7948.
(63) (a) Koenig, T.; Wielesek, R. A.; Huntington, J. G. *Tetrahedron Lett.* **1974,** 2283. (b) Koenig, T. Personal communication.
(64) Shelton, J. R.; Uzelmeier, C. W. *J. Am. Chem. Soc.* **1966,** *88,* 5222.
(65) McDonald, R. N.; Reitz, R. R. *J. Am. Chem. Soc.* **1976,** *98,* 8144.
(66) Shono, T.; Nishiguchi, I. *Tetrahedron* **1974,** *30,* 2183.
(67) Stefani, A. P.; Chuang, L.-Y.; Todd, H. E. *J. Am. Chem. Soc.* **1970,** *92,* 4168.
(68) Fort, R. C., Jr.; Hiti, J. *J. Org. Chem.* **1977,** *42,* 3968.
(69) Ernst, J. A.; Thankachan, C.; Tidwell, T. T. *J. Org. Chem.* **1974,** *39,* 3614.
(70) Timberlake, J. W.; Garner, A. W. *J. Org. Chem.* **1976,** *41,* 1666.
(71) Friedman, R. L.; Lewis, R. N.; Pastorino, R. L. *Mod. Plast.* **1971,** 66.
(72) Garner, A. W.; Timberlake, T. W.; Engel, P. S.; Melaugh, R. A. *J. Am. Chem. Soc.* **1975,** *97,* 7377.
(73) (a) Duismann, W.; Rüchardt, C. *Tetrahedron Lett.* **1974,** 4517. (b) *Chem. Ber.* **1973,** *106,* 1083.
(74) Griller, D.; Ingold, K. U. *Acc. Chem. Res.* **1976,** *9,* 13.
(75) Porter, N. A.; Dubay, G. R.; Green, J. G. *J. Am. Chem. Soc.* **1978,** 100, 920,

and references cited therein.
(76) Engle, P. S.; Bishop, D. J. *J. Am. Chem. Soc.* **1975,** 97, 6754.
(77) Nozaki, K.; Bartlett, P. D. *J. Am. Chem. Soc.* **1946,** *68,* 1686.
(78) Tang, F.; Huyser, E. S. *J. Org. Chem.* **1978,** *43,* 1016.
(79) Russell, G. A. in ref 12, p 312.
(80) (a) Kozuka, S.; Lewis, E. S. *J. Am. Chem. Soc.* **1976,** *98,* 2254. (b) Lewis, E. S.; Ogino, D. *ibid.* **1976,** *98,* 2264.
(81) Milas, N. A.; Golubovic, A. *J. Am. Chem. Soc.* **1958,** *80,* 5994.
(82) Rüchardt, C.; Schwarzer, H. *Chem. Ber.* **1966,** *99,* 1861.
(83) Pryor, W. A.; Kneipp, K. G. *J. Am. Chem. Soc.* **1971,** *93,* 5584.
(84) We thank Dr. Sal Rand of the Texaco Research Center, Beacon, N.Y., for taking the 100-MHz spectra for us.
(85) Koenig, T.; Wolf, R. *J. Am. Chem. Soc.* **1967,** *89,* 2948.
(86) "The Aldrich Catalog-Handbook of Organic and Biochemicals", Aldrich Chemical Co., Inc.: Milwaukee, Wis., 1977–1978.
(87) Gassman, P. G.; Heckert, D. C. *Tetrahedron* **1965,** *21,* 2725.
(88) Pratt, D. G.; Rothstein, E. *J. Chem. Soc. C* **1968,** 2548.
(89) Atkinson, J. G.; Csakvary, J. J.; Herbert, G. T.; Stuart, R. S. *J. Am. Chem. Soc.* **1968,** *90,* 498.
(90) Vogel, A. I. "A Textbook of Practical Organic Chemistry", Longman: London, 1956; p 859.
(91) Abell, P. I.; Tien, R. *J. Org. Chem.* **1965,** *30,* 4212.
(92) Haworth, E.; Perkin, W. H. *J. Chem. Soc.* **1894,** *65,* 86.
(93) Walker, H. G.; Hauser, C. R. *J. Am. Chem. Soc.* **1946,** *68,* 1386.
(94) Simmons, H. E.; Blanchard, E. P.; Smith, R. D. *J. Am. Chem. Soc.* **1964,** *86,* 134.
(95) Cox, E. F.; Caserio, M. C.; Silver, M. S.; Roberts, J. D. *J. Am. Chem. Soc.* **1961,** *83,* 2719.
(96) Reference 86, p 211.
(97) Reference 86, p 222.
(98) Reference 86, p 215.

Epimerization and Isomerization in C$_{20}$ Diterpenoid Alkaloids. Crystal and Molecular Structures of Atisinium Chloride, Dihydroatisine, Isoatisine, and Veatchine[1]

S. William Pelletier,* Wilson H. De Camp, and Naresh V. Mody

Contribution from the Institute for Natural Products Research and Department of Chemistry, University of Georgia, Athens, Georgia 30602. Received April 17, 1978

Abstract: The solid-state conformation of four C$_{20}$ diterpenoid alkaloids has been determined by X-ray crystallography. Atisinium chloride (orthorhombic, $P2_12_12_1$, $a = 14.340$, $b = 18.180$, $c = 7.709$ Å, $R = 0.038$ for 2007 observed reflections) is shown to have restricted access to both sides of the iminium double bond. Dihydroatisine (orthorhombic, $P2_12_12_1$, $a = 13.004$, $b = 18.939$, $c = 7.840$ Å, $R = 0.055$ for 1651 observed reflections) is shown to have a chair conformation for ring E, thus giving a basis for assignment of all ^{1}H and ^{13}C NMR resonances, and showing that boat-chair conformational isomerism of ring E is unlikely. Isoatisine (orthorhombic, $P2_12_12_1$, $a = 13.212$, $b = 13.661$, $c = 10.403$ Å, $R = 0.048$ for 1945 observed reflections) shows that the oxazolidine ring F closes exclusively in the endo configuration when closure is in the iso form. This result confirms a ^{13}C NMR study that isoatisine does not exist as a pair of epimers. Furthermore, it indicates that the doubled signal of the C(4) methyl group in isoatisine is attributable neither to a mixture of C(19) epimers, as was suggested in the case of atisine, nor to a mixture of the chair and boat conformers of the piperidine ring E. Veatchine (orthorhombic, $P2_12_12_1$, $a = 9.934$, $b = 21.581$, $c = 8.674$ Å, $R = 0.050$ for 1614 observed reflections) reveals a crystal structure which is disordered between C(20) epimers, showing that the normal closure of the oxazolidine ring can take place on either side of the iminium double bond, in agreement with the observed ^{13}C NMR data. The absolute configuration of atisinium chloride is shown to be $4S,5S,8R,10R,12R,15S$ by the R-ratio test. By analogy, the absolute configuration of dihydroatisine must be $4S,5S,8R,10R,12R,15S$, and that of isoatisine must be $4S,5S,8R,10R,12R,15S,19S$. The absolute configuration of veatchine must be $4S,5S,8R,10R,13R,15R,20SR$, with the SR indicating a predominance of the 20S epimer. A similar configuration at C(20) is postulated for atisine on the basis of spectral data. The $S:R$ ratio in veatchine is approximately 60:40, based on measurements of the diffracted intensity for sensitive reflections, which is in substantial agreement with the ratio found by integrating the C(4) methyl resonance in the ^{1}H NMR spectra of the two different sets of ^{13}C chemical shifts for the carbon atoms of the oxazolidine ring, piperidine ring, and C(4) methyl group.

Introduction

The C$_{20}$ diterpenoid alkaloids isolated from various *Aconitum* and *Garrya* species (principally *A. heterophyllum* Wall, *G. veatchii* Kellogg, and *G. lauifolia* Hartw.) have been the subjects of extensive chemical investigation.[2-4] The molecular structure and stereochemistry of atisine (1) and several related alkaloids were initially established by classical degradative and synthetic methods.[2-4] Atisine (1), an amorphous base (pK_a =

12.8), undergoes a facile isomerization of the oxazolidine ring F (see Experimental Section for ring definitions) from its "normal" position (closed on C(20)) to the "iso" position (closed on C(19)) of isoatisine (2) by treatment with methanolic alkali or even by simple refluxing in hydroxylic solvents.[5] The path of this isomerization presumably goes through the ternary iminium form (3), which tautomerizes to the isoiminium form (4). The isomerization can be reversed by refluxing